IEEE Access
Multidisciplinary | Rapid Review | Open Access Journal

Received September 6, 2021, accepted September 14, 2021, date of publication September 16, 2021,
date of current version September 30, 2021.

Digital Object Identifier 10.1109/ACCESS.2021.3113566

A Precise Lesion Localization System Using a Magnetometer With Real-Time Baseline Cancellation for Laparoscopic Surgery

SOON-JAE KWEON[1,2], (Member, IEEE), WOOJIN YUN[3,4], HYUNWOO PARK[2], (Student Member, IEEE), JEONG-HO PARK[2,5], JUNG HOON LEE[6], (Member, IEEE), JIN LEE[7], MINKYU JE[2], (Senior Member, IEEE), SOHMYUNG HA[1,8], (Senior Member, IEEE), AND CHOUL-YOUNG KIM[4], (Member, IEEE)

[1]Division of Engineering, New York University Abu Dhabi, Abu Dhabi, United Arab Emirates
[2]School of Electrical Engineering, Korea Advanced Institute of Science and Technology, Daejeon 34141, Republic of Korea
[3]National Nanofab Center, Daejeon 34141, Republic of Korea
[4]Department of Electronics Engineering, Chungnam National University, Daejeon 34134, Republic of Korea
[5]System LSI Business, Samsung Electronics Company Ltd., Hwaseong-si, Gyeonggi-do 18848, Republic of Korea
[6]Department of Electronics Engineering and Applied Communications Research Center, Hankuk University of Foreign Studies, Yongin 17035, Republic of Korea
[7]Department of Information and Communication, Pyeongtaek University, Pyeongtaek 17869, Republic of Korea
[8]Tandon School of Engineering, New York University, New York, NY 10003, USA

Corresponding authors: Sohmyung Ha (sohmyung@nyu.edu) and Choul-Young Kim (cykim@cnu.ac.kr)

This work was supported in part by the Commercialization Promotion Agency for Research and Development Outcomes (Research Equipment Development-01-1 Program), in part by the Information Technology Research Center (ITRC) Program through the Institute of Information and Communications Technology Planning & Evaluation (IITP) under Grant IITP-2020-0-01778, in part by the Ministry of Science and ICT (MSIT), Republic of Korea, and in part by the Basic Science Research Program through the National Research Foundation of Korea (NRF) funded by the Ministry of Education, Republic of Korea, under Grant 2021R1A6A3A03043927.

ABSTRACT Laparoscopic surgery is a technique in which surgeons insert laparoscopic instruments into the body through a small incision and conduct surgical operations. It offers a shorter recovery period, less blood loss, and less postoperative pain than open surgeries. In order to maximize these benefits of this surgery technique, it is important to localize the lesion accurately without palpation, minimizing the surgical area. It is because surgeons cannot palpate the organ during laparoscopic surgeries. For accurate localization, we propose a lesion localization system (LLS). This adopts an endoscopic clip with a small-size magnet as a marker and an improved magnetometer as a probe for measuring the magnetic field from the magnet. The magnetometer, which consists of two Hall sensors, can cancel out the fluctuating magnetic baseline mainly caused by external environments so that it can detect a smaller change in the target magnetic field. As a result, the LLS improves the detection range up to 40 mm while using a weak magnet with a small volume of 17.1 mm^3, which is compatible with the use of commercial clip appliers. An error of less than 0.1% is achieved at a distance of 40 mm, and the maximum error is kept below 6% even when the rotation angle is varied to $\pm 90°$. This LLS does not cause discomfort to the surgery operation because it uses a marker small enough and does not require external coils.

INDEX TERMS Baseline cancellation, endoscopic clip, hall sensor, laparoscopic surgery, lesion localization, magnetometer, minimally invasive surgery, precision, small-sized magnet.

I. INTRODUCTION

Minimally invasive surgeries (MISs) have become a preferred surgery method over conventional open surgeries, allowing the surgeon to access the internal organs through small incisions [1]. MISs have been widely adopted in various fields of surgery with rapid developments [2]–[4]. Particularly, laparoscopic surgeries, one of the MISs, have been applied for gastrointestinal surgeries and have advanced with the development of various surgical instruments [5], [6]. In laparoscopic surgeries, surgeons insert laparoscopic instruments into the body through a small incision and conduct complex

The associate editor coordinating the review of this manuscript and approving it for publication was Wenbing Zhao.

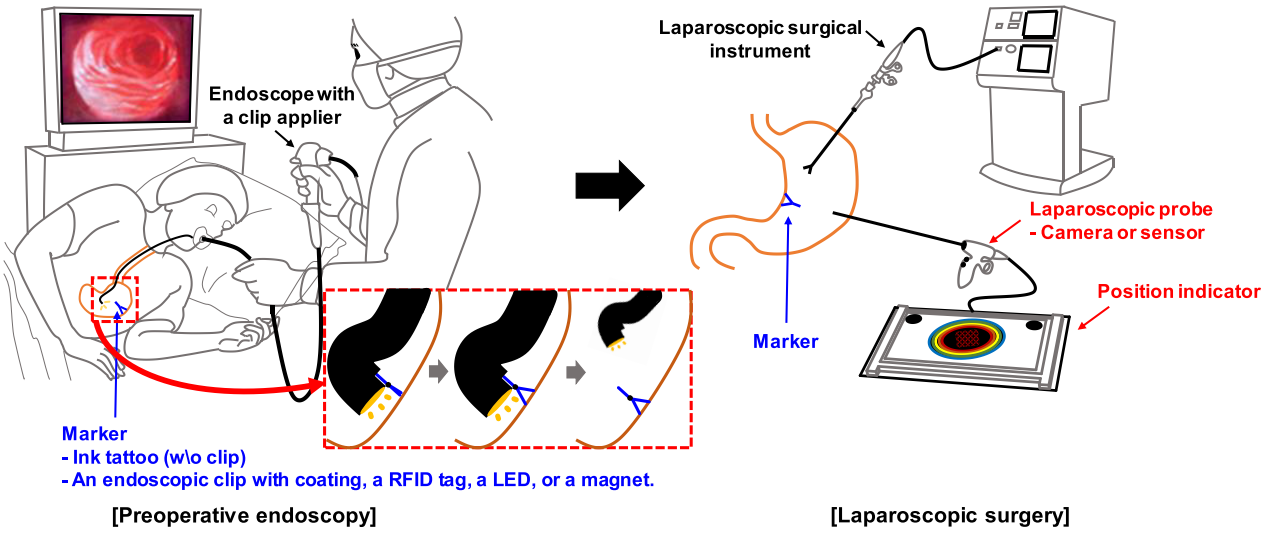

FIGURE 1. A surgical procedure using a lesion localization system for laparoscopic surgery.

operations within the chest cavity, abdomen, or pelvis [7]. This results in a shorter recovery period, less blood loss, less severe postoperative pain, and better cosmetic outcomes compared to open surgeries [5]–[9].

Although laparoscopic surgeries are beneficial to patients, there are some challenges. One of the main challenges is that it is difficult for the surgeon to localize the small lesion, such as early cancer, because they cannot palpate the organ [5]. If the lesion is inaccurately localized, a further laparotomy is necessary to respect the remaining lesion [10]. Therefore, it is important to localize the lesion accurately during the surgery to determine the correct oncologic resection range [5], [11]. As one of the conventional marking methods, an endoscopic clip can be attached near the lesion by an endoscopic clip applier during a preoperative endoscopy. Since the clips are invisible from the outside of the serosal walls, however, the surgeon needs to palpate to localize the clips [5], [12]. Therefore, several localization systems have been proposed for laparoscopic surgery to localize the lesion accurately without palpation.

Fig. 1 shows a surgical procedure using a lesion localization system (LLS) for laparoscopic surgery. During the preoperative endoscopy process, a marker is attached or tattooed to the target lesion. When the marker is made based on advanced techniques, a clip applier is used to inject the marker through the working channel while localizing the tumor by using the camera of the endoscope. Since the working channel of conventional endoscopes has a diameter of 2.8 mm [13], the marker should have a diameter less than that of the working channel to be inserted without other equipment. In the following laparoscopic surgery process, the marker is identified by a laparoscopic probe (LP), and then the lesion is resected or treated by laparoscopic surgical instruments. Here the LP should have a diameter of less than 10 mm to insert the LP through a 10-mm laparoscopy trocar port. It is in great demand for a small marker and a precise localization method with small and simple hardware.

One of the popular conventional marking methods is tattooing. India ink is injected near the target lesion during the preoperative endoscopy or the first diagnostic endoscopy [14]–[16]. The target lesion's location can be identified during laparoscopic surgery because India ink can be visible outside the organ. However, several problems were reported; this method would cause inflammation, perforation, or inaccurate marking by washout and spreading of the ink [5], [6], [17], [18]. Although safety-related issues can be resolved by using the indocyanine green ink instead of India ink [19], this method using indocyanine green has not resolved the inaccurate marking issue by ink spreading [5]. Subsequently, endoscopic clips coated with indocyanine green or other fluorescent dyes have been proposed to avoid the spreading of the ink [20]–[22]. However, this method requires a special light, cameras, or eyewear to identify the fluorescent ink [18], [20].

As IT technologies advance rapidly, several types of LLSs combining with various IT technologies have been proposed to overcome the drawbacks of ink-based LLSs. It was proposed to use an endoscopic clip attached with a radio frequency identification (RFID) tag as a marker [6], [12], [13]. The antenna in the corresponding LP supplies power to the tag in the organ while the LP detects the signal strength transmitted from the tag. The tag and the antenna are small enough to use a commercial endoscopic-clip applier and a 10-mm laparoscopy trocar port. For example, the RFID tag in [6] has a radius of 2.23 mm and a thickness of 9 mm, and it was attached to the lesion with an endoscopic clip as a maker. And an antenna with a radius of 9 mm was used for localization [6]. However, these LLSs have a limited detection range due to the small size of antennas. The communication range between the tag and the antenna

decreases as the antenna gain decreases [23]–[25]. The LLS in [6] achieved a detection range of less than 22 mm. In order to increase the detection range, a thoracoscopic surgery support system using one more antenna was proposed [26]. Here the antenna inside the LP only detects the signal while an additional antenna outside the body supplies power to the RFID tag. This LLS achieved an improved detection range of less than 30 mm by using the power-supplying antenna. However, it could cause discomfort during the surgery because the additional antenna should be placed just outside the lesion to transmit the power.

Alternatively, an LLS with an endoscopic clip that employs a light-emitting diode (LED) and a small coiled antenna as a marker was proposed [5]. The marker with the LED and antenna has a radius of 2 mm and a thickness of 9 mm. Due to this LED, the location of the clip can be identified by a laparoscopic camera during surgery. Here, power for the LED is delivered through the coiled antenna from an external power source outside the body. To supply sufficient power, the external power source should be placed close to the surgery region of the patient. Although the external power source using a coiled antenna of 200-mm diameter is smaller than the additional antenna in [26], it may still cause discomfort to the surgeons during surgery. When insufficient power is provided to the LED due to a long distance or an unmatched direction between two antennas, the LED may not be turned on, leading to a failure of lesion localizing.

To avoid using additional external devices such as antennas, an LLS using a magnet and a magnetometer was proposed [27]. A magnet is attached to the endoscopic clip, which is placed near the lesion during preoperative endoscopy. The magnetometer on the LP measures the magnitude of the B field from the magnet to localize the clip. In a clinical study using a magnet with a maximum B-field magnitude of 320-mT and a magnetometer with 10-mT detecting ability, this LLS achieved a detection rate of 100% and 40% at distances of 10 mm and 50 mm, respectively [27]. However, this LLS's detection rate and range decrease as the marker's maximum B-field magnitude decreases. For example, the detection rate of 40% at 50 mm was reduced to 0% when a smaller magnet with a maximum B-field magnitude of 130-mT was used. The maximum B-field magnitude is determined by the dimension of the marker. The size of the magnet is firstly limited by the commercial clip applier, which is used to inject the magnet and the endoscopic clip into the organ. Thus, with a given small size of the magnetic marker, the detecting ability of the magnetometer should be improved to achieve a better detection rate and range.

To address this challenge, this paper proposes an LLS that achieves a longer detection range with high precision by using an improved magnetometer. The proposed magnetometer consists of two Hall sensors to detect a much smaller B-field change differentially by removing fluctuating baselines mainly caused by external environments in real-time. As a result, the proposed LLS can improve the detection range while using a much weaker and smaller magnet, which is more suitable for using commercial clip appliers. The conventional LLS based on a magnetometer in [27] had difficulty in the attachment process because the diameter of the magnet is larger than the working channel of conventional endoscopes [13]. The diameter of its magnet is 4 mm [27], whereas the diameter of the working channel of conventional endoscopes is 2.8 mm [13]. On the contrary, the magnet adopted in the proposed LLS has a diameter of 2.2 mm, which is smaller than the working channel. Furthermore, the longer detection range of the proposed LLS would be helpful for localizing the tumor more quickly. The commercial Hall sensors on the magnetometer have a sufficient sensitivity with a small form factor.

The proposed LLS has the following advantages compared to other types of LLSs. The proposed LLS does not have the inaccurate marking issue by ink spreading or the safety issue, both of which are the main concerns of ink-based LLSs. According to the clinical results in [27], none of the patients experienced complications from the magnetometer-based LLS. Next, the proposed LLS does not require high-cost external equipment like a special light or camera which are required in LLSs based on ink-coated endoscopic clips. At last, the proposed LLS does not employ any external antenna, which is required in the RFID-based LLS and LED-based LLS. The proposed LLS achieves an even longer detection range than the RFID-based LLS without the discomfort caused by the antenna. In addition, it does not have the localization-failure issue of LED-based ones because it does not require any external power supply for the clip.

The remainder of this paper is organized as follows. Section II discusses the main challenges in detecting small B fields in surgery room environments. Section III describes the hardware implementation and the algorithm of the proposed LLS. Section IV presents measurement results of the system, followed by conclusions in Section V.

II. CHALLENGES IN MEASURING SMALL MAGNETIC FIELDS

The B field from the magnet of the marker is too small to be easily interfered by other magnetic fields from the surrounding environment. The ambient environment magnetic field (B_{env}) is a combination of a geomagnetic field (B_{geo}) and a B field from ferromagnetic objects (B_{ferro}) nearby [28]. This makes an unwanted baseline in the B field of the LP, interfering with the small B field from the marker indicating the target lesion's location.

B_{geo} has a constant magnitude within a range from 23 μT to 66 μT and a fixed direction if confined in a small-scale region [29]. Therefore, the magnitude of B_{geo} ($|B_{geo}|$) can be compensated by measuring $|B_{geo}|$ with and without the magnet and taking the difference. However, this process may cause inconvenience for surgeons to some extent and does not work well for cases with long surgery time. Moreover, the magnitude of B_{env} ($|B_{env}|$) fluctuates not only by various environment conditions such as surrounding objects and time

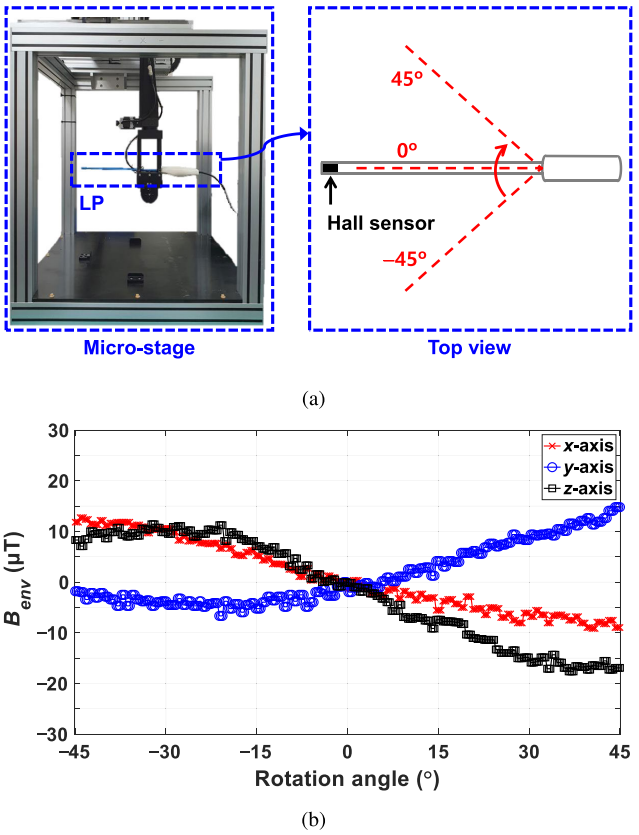

FIGURE 2. **(a) Experiment setup for measuring the ambient magnetic field (B_{env}) with varying rotation angle of the LP. The LP is rotated from −45° to 45°. (b) B_{env} output of the Hall sensor. The data of each axis are calibrated by subtracting the measurement value at 0° from the measurement outputs.**

but also by the vertical and horizontal positions and angles of the LP [28]–[33]. The LP should be moved constantly to localize the lesion, and the positions of surrounding electrical instruments can be changed during the surgery. Thus, it is difficult to compensate for such fluctuations by using an initial background B_{env} measurement. Therefore, these fluctuating baselines should be automatically removed in real-time because it is not practical to calibrate periodically during surgery.

To observe the fluctuation of B_{env} according to the movement of the LP, the magnetic field was measured with the B-field-sensing LP in the experiment setup shown in Fig. 2(a). The LP has a Hall sensor at the inner end and was fixed to a micro-stage. The LP was rotated in the micro-stage from –45° to 45° with no magnet nearby while it was kept parallel to the floor. Fig. 2(b) shows the measured results of B_{env} in the x-, y-, and z-axes. The B_{env} measurements of the three axes were calibrated by subtracting the measurement value at 0° from the measurement outputs. As shown in the figure, the measured B fields significantly fluctuate as the rotation angle changes. This fluctuating baseline by the rotation of the LP cannot be removed by the initial calibration. Whenever the rotation angle changes, this varying baseline is measured, which interferes with the measurement of the target B field from the magnet of the marker.

III. PROPOSED LESION LOCALIZATION SYSTEM

The proposed LLS consists of a marker, an LP, and a position indicator, as shown in Fig. 1. Among various markers, the proposed LLS adopts an endoscopic clip with a magnet. This kind of markers does not involve the inaccurate marking issue by spreading of ink. In addition, the marker does not need to receive power using an antenna or from a battery.

Fig. 3(a) shows a block diagram of the magnetometer, which is embedded at the inner end of the LP and the signal processor inside the position indicator of the proposed LLS. Fig. 3(b) shows pictures of the LP, the magnetometer inside the LP, the position indicator, and the signal processor board. Since only a tiny volume is allowed inside the LP, the magnetometer consists of only two Hall sensors and several passive components, including decoupling capacitors, to minimize the volume. The magnetometer measures the surrounding B field while the signal processor performs all other processing functions. The Hall sensors (MPU-9250, InvenSense), which include an integrated analog-to-digital converter (ADC), have a sensitivity of 0.6-μT LSB and a full-scale range of $\pm$4800 μT with a small size of 3.0 × 3.0 × 1.0 mm^3. Other analog-output Hall sensors may have a wider range and better sensitivity, but they require external amplifiers and high-resolution ADCs. This requires a large board area, so it is not suitable for small magnetometers. ATMEGA2560 is used as a microcontroller of the signal processor. It transmits commands to the magnetometer, receives digital data from the magnetometer through I^{2}C communication, and indicates the distance using an LCD monitor and a buzzer. As shown in Fig. 3(c), the LCD monitor changes according to the distance between the LP and the marker. A DC-DC converter and a low-dropout (LDO) regulator generate the supply voltages for the whole system. Using a USB-to-UART interface, the firmware of the microcontroller can be updated, and the collected data can be sent to the computer.

The proposed magnetometer consists of two Hall sensors ($SENSOR_1$ and $SENSOR_2$) to remove any fluctuating B_{env} baseline in real-time. As shown in Fig. 3(b), $SENSOR_1$ is located at the end of the LP, and the $SENSOR_2$ is located 40 mm apart from $SENSOR_1$. When the LP is near the marker, $SENSOR_1$ simultaneously measures a B field generated by the magnet (B_{magnet}) and B_{env}. $SENSOR_2$ also measures B_{env} and B_{magnet}, but B_{magnet} measured by $SENSOR_2$ is much smaller because of the two sensors' position. The microcontroller subtracts the measured outputs of $SENSOR_2$ from those of $SENSOR_1$ by using the following equation:

$$\Delta = \sqrt{(B_{x1} - B_{x2})^2 + (B_{y1} - B_{y2})^2 + (B_{z1} - B_{z2})^2} \quad (1)$$

where B_{x1}, B_{y1}, and B_{z1} are measured outputs in x, y, and z directions of $SENSOR_1$ after an offset cancellation,

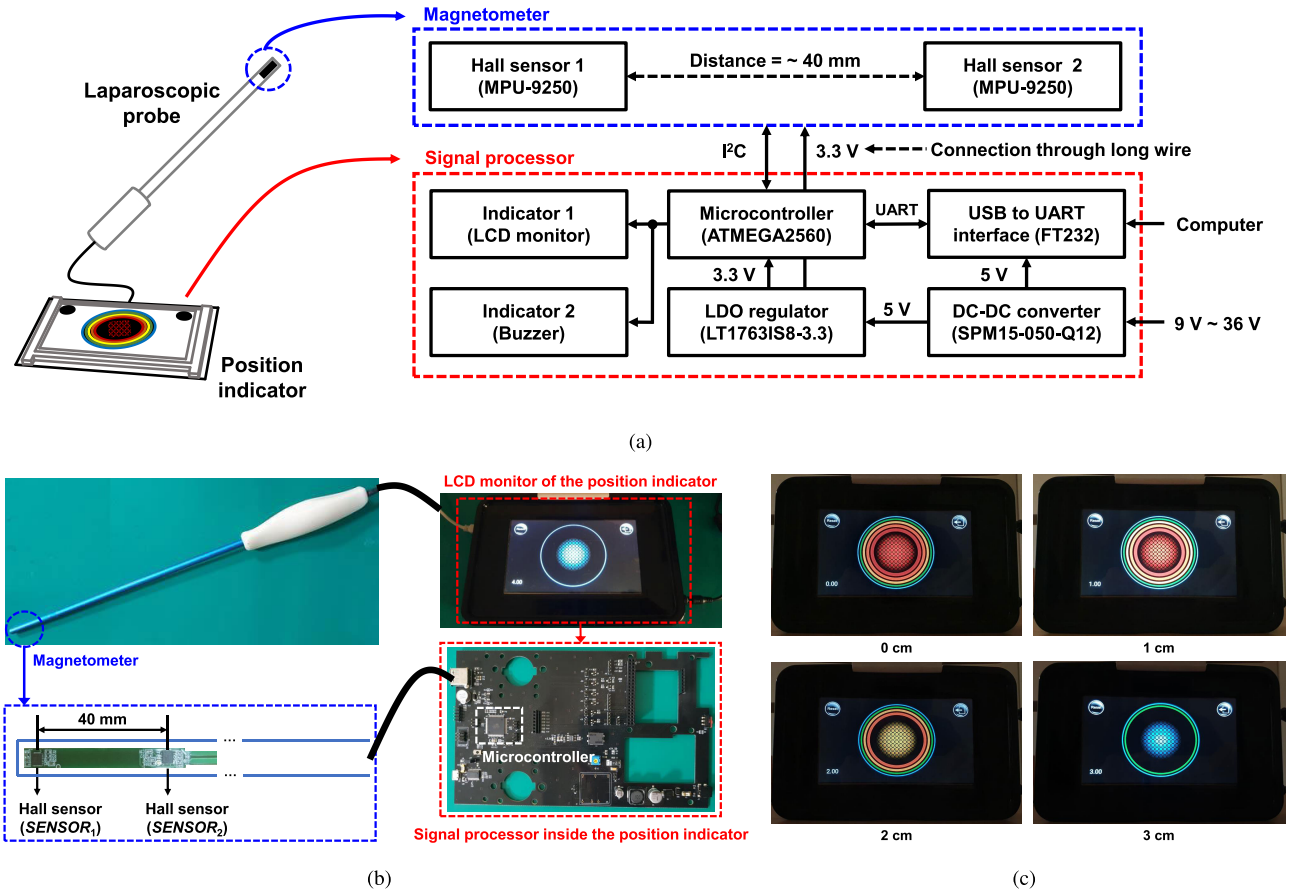

FIGURE 3. (a) A block diagram of the magnetometer, which is embedded at the inner end of the LP, and the signal processor inside the position indicator of the proposed LLS. (b) Pictures of the prototype: LP (top left), magnetometer board (bottom left), position indicator (top right), and signal processor board (bottom right). (c) Position indicator displaying the distance of 0, 1, 2, and 3 cm.

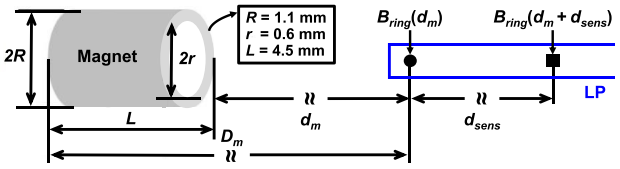

FIGURE 4. Simplified configuration for calculation of the *B* field from a ring-type magnet.

TABLE 1. The ratio between *B* fields at two different locations.

d_m (mm)	d_{sens} (mm)	$\lvert B(d_m + d_{sens})\rvert / \lvert B(d_m)\rvert$
40	10	0.52
40	20	0.31
40	30	0.19
40	40	0.13
40	50	0.09

respectively. B_{x2}, B_{y2}, and B_{z2} are results of $SENSOR_2$. Δ is converted to the distance between the magnet and the LP by using a look-up table.

The closer the distance between $SENSOR_1$ and $SENSOR_2$ (d_{sens}) gets, the more effectively B_{env} is cancelled out. It is because two sensors receive more identical B_{env} from the surrounding environments. However, if d_{sens} is too close, B_{magnet} is also cancelled out. Thus, d_{sens} should be large enough for B_{magnet} measurement. The magnitude of the B field can be calculated using the Biot-Savart law in order to determine d_{sens}. Assume a ring-type magnet shown in Fig. 4, which is suitable to be attached to the endoscopic clip. The magnitude of the B field generated by the magnet at d_m is given as follows [34]:

$$|B_{ring}(d_m)| = \frac{B_r}{2} \times \left[\left(\frac{D_m}{\sqrt{R^2 + D_m^2}} - \frac{D_m}{\sqrt{r^2 + D_m^2}} \right) - \left(\frac{d_m}{\sqrt{R^2 + d_m^2}} - \frac{d_m}{\sqrt{r^2 + d_m^2}} \right) \right] \quad (2)$$

where B_r is a residual magnetic flux density depending on the material of the magnet. This is the value when an external field is not existed. Table 1 shows the ratio between magnitudes of B fields at d_m and $d_m + d_{sens}$ obtained by Eq. (2). When d_{sens} is longer than 30 mm, $|B_{magnet}|$ measured by $SENSOR_2$ at $d_m + d_{sens}$ ($|B(d_m + d_{sens})|$) can be smaller than 20% $|B_{magnet}|$ measured by $SENSOR_1$ at d_m. Based on

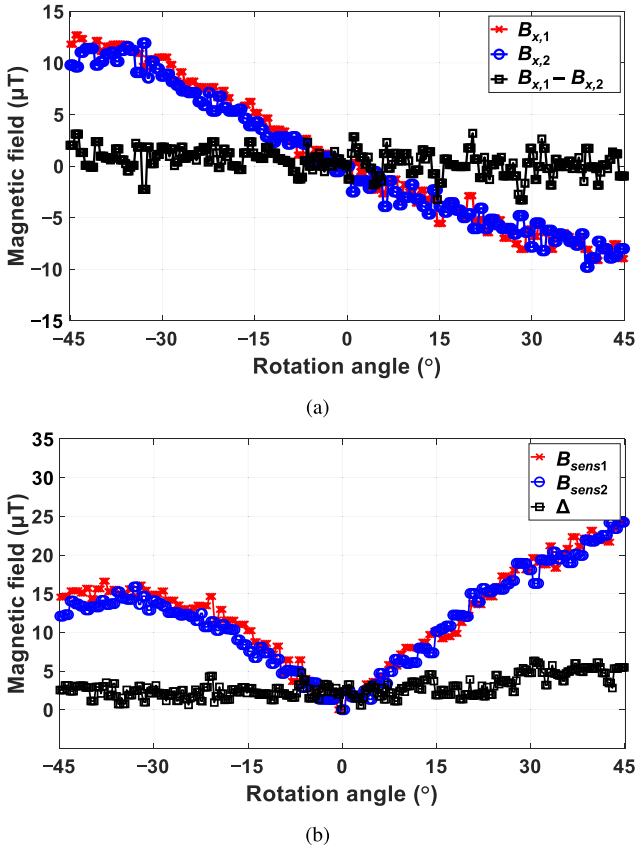

FIGURE 5. Baseline cancellation results for (a) *x*-axis and (b) magnitude of *B* field when the LP is rotated from −45° to 45°.

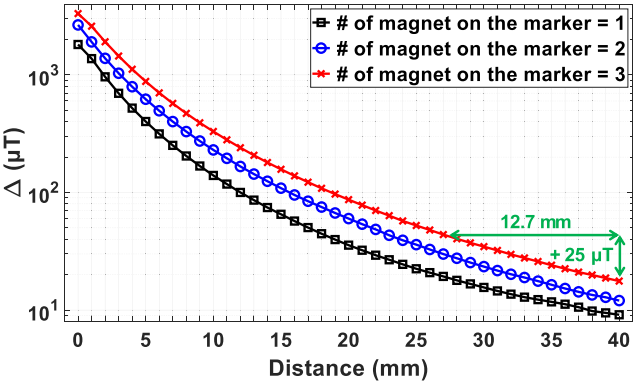

FIGURE 6. Measured Δ (the magnetic field difference) over d_m (the distance between the LP and the marker) for three different number of unit magnets.

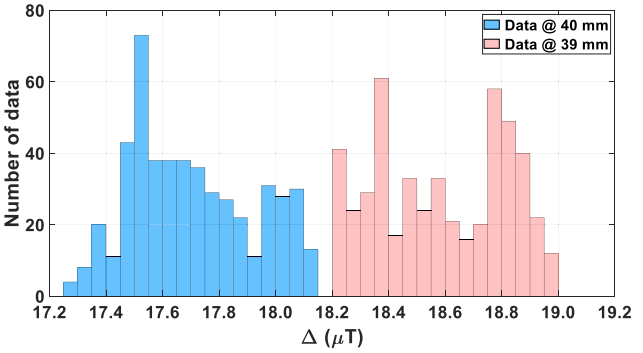

FIGURE 7. Histogram of measured Δ for distances at 40 mm and 39 mm. Here 100 samples are averaged for each data point.

this with a design margin, d_{sens} of the prototype was set to be 40 mm.

IV. MEASUREMENT RESULTS

This section presents the experimental results about the baseline cancellation and detection range of the proposed LLS. The LP and the position indicator of the prototype shown in Fig. 3(b) and (c) were used to detect the distance between the LP and an endoscopic clip with a ring-type magnet.

The same experiments shown in Fig. 2 with the magnetometer were performed to validate the real-time baseline cancellation. Fig. 5(a) shows B_{x1} and B_{x2} measured by $SENSOR_1$ and $SENSOR_2$, respectively. The micro-stage rotated the LP from –45° to 45° while keeping it parallel to the floor. Both B_{x1} and B_{x2} significantly fluctuate as the rotation angle changes. However, $B_{x1} - B_{x2}$ remains almost constant regardless of the rotation angle. Fig. 5(b) shows Δ (Eq. (1)) of $|B_{sens1}|$ and $|B_{sens2}|$, which are the B fields measured by $SENSOR_1$ and $SENSOR_2$ after calibration to the angle 0°. As shown, the fluctuation of Δ is significantly reduced from 25 μT to less than about 6 μT across the rotation angle range.

This remaining baseline Δ limits the sensitivity of the magnetometer. To ensure sound measurements, Δ from the marker should be larger than this remaining baseline. Fig. 6 shows Δ measured by the LP over the distance d_m. Here, the number of unit magnets on the marker is changed from one to three. The unit ring-type magnet has a dimension of $R = 1.1$ mm, $r = 0.6$ mm, and $L = 1.5$ mm. As d_m increases, Δ decreases. All across the distance range of interest (40 mm), Δ is always higher than 6 μT. Because one magnet consisting of three unit magnets is still small enough and gives a higher B field, we determined to use three unit magnets. The dimension of the magnet is still smaller than the RFID tag in [6] and the LED with the coiled antenna in [13]. The beneficial effect from the baseline cancellation increases as d_m increases. For example, when 25 μT, which is the maximum value of measured baseline in Fig. 5(b), is added to the data at 40 mm due to lack of the baseline cancellation, the data at 40 mm cannot be distinguished from the data at 27.3 mm. When 15 μT, which is the minimum value of measured baseline, is added, the data at 40 mm is difficult to be differentiated from the data at 30.8 mm. As such, the baseline can interfere with the detection severely when d_m is large. Thanks to the baseline cancellation technique, detection at long d_m can be significantly improved, thus extending the maximum detection range.

Fig. 7 shows a histogram of the measured Δ for two different distances, 39 mm and 40 mm. Each data was

TABLE 2. Performance summary and comparison.

	This work	[27]	[6]	[26]	[5]
Marker	Clip with a 3.2-mT magnet	Clip with a 320-mT magnet	Clip with a RFID tag	Clip with a RFID tag	Clip with an LED
Marker volume	17.1 mm^3	25.1 mm^3	35.8 mm^3	27.7 mm^3	28.3 mm^3
Sensors in LP	Hall sensors	Hall sensor	Antenna	Antenna	Camera
External devices	No	No	No	Coil surrounding the chest	Coil with radius of 200 mm
Detection range	$>$ 40 mm	50 mm with 40% detection rate	7 mm to 22 mm	30 mm	N/A
Accuracy	Error rate $<$ 0.1% with fixed angle Error rate $<$ 6% with different angles	Detection rate = 0% at 10 mm with 80-mT magnet	N/A	N/A	N/A

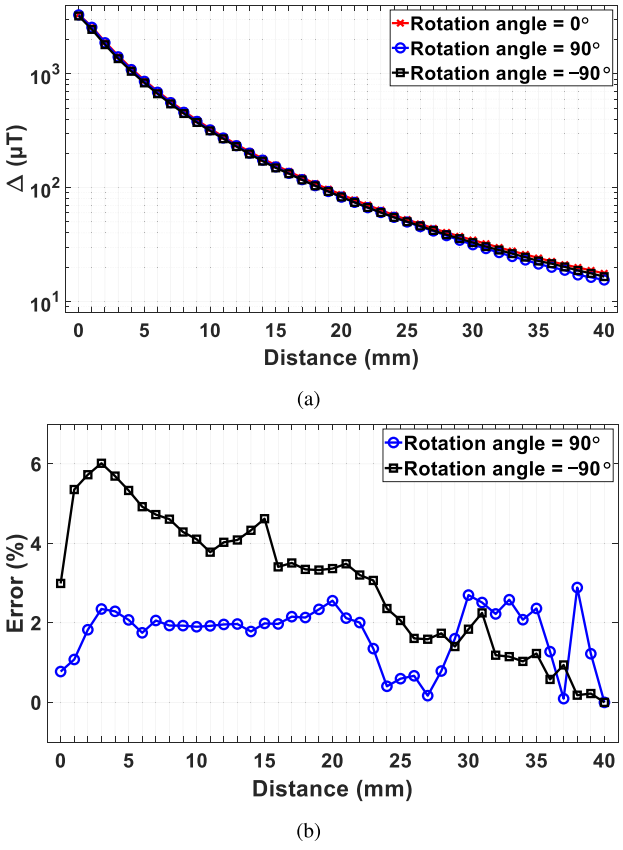

FIGURE 8. (a) Δ and (b) error over d_m of the LP for different rotation angles.

obtained by averaging 100 samples. When the number of average, N_{avg}, is higher than 100, 500 data at 40 mm and 500 data at 39 mm are completely distinguishable from each other without error. This infers that the bit-error rate (BER) for 1 mm resolution is lower than 0.2%. To perform this average function, a data storage of $3 \times 2 \times N_{avg} \times 2$ bytes of is required. It is because Δ in Eq. (1) is obtained from three axes of two sensors, and each data has a size of 2 bytes. This amount of storage can be easily provided by the microcontroller (ATMEGA2560), which includes an 8-Kbyte SRAM.

Fig. 8(a) shows Δ for three different rotation angles of the LP, *i.e.*, 0°, 90° and –90°. For different rotation angles, the baseline is different, as shown in Fig. 5. Thanks to the baseline cancellation, the baseline is removed, so all these three Δs have a good agreement. Fig. 8(b) shows the Δ error of the cases with rotation angles of –90° and 90° compared to Δ at 0°. Δs at 40 mm of three cases are calibrated for removing the offsets caused by inaccurate positioning during experiments. The maximum error is only 6%. It is important to know not only the location of the tumor but also the precise distance between the tumor and the LP because the operator needs to resect the tumor with a clinical margin accurately. The marginal resection range may depend on the operator and has been reported with a wide range [6]. The National Comprehensive Cancer Network (NCCN) suggests a margin of 40 mm or greater than the gross tumor [35]. The Japanese Gastric Cancer Association (JGCA) suggests a margin of 20–30 mm for early gastric cancers [36]. In this regard, the baseline cancellation can be helpful to precisely resect the tumor with such margin, thanks to the increased detection range. The detection range up to 40 mm meets both guidelines of NCCN and JCGA [35], [36].

The performances of the proposed LLS and other previous LLSs are summarized and compared in Table 2. An endoscopic clip with a magnet, which has a 3.2-mT maximum magnitude of B_{magnet}, is used as a marker in this work. The proposed magnetometer cancels out the fluctuating baseline by utilizing two Hall sensors. A detection error of less than 0.1% was achieved at a distance of 40 mm. The maximum error is only 6% when the rotation angle is at –90°. Compared to the previous LLS using a magnet [27], the proposed LLS achieved an improved detection range even with a much weaker magnet. This means that the magnet of the proposed LLS can be a much smaller size than that of the LLS in [27] when the magnets are composed of the same material and have the same B_r (Eq. (2)). The proposed LLS achieves a longer detection range of 40 mm than other LLSs in [6] and [26] based on RFID tags. It is because the detection range does not depend on the dimension of the antenna inside of the LP. In addition, the proposed LLS does not need a battery in the marker unlike [5], enabling a small marker size. The volume of our marker except the clip is compared to those of

others, and it is the smallest. Moreover, it does not require any external coil, which is likely to disturb the operation during surgery unlike [5], [26].

Some magneto-based localization systems have been developed for capsule endoscope localization by measuring the magnetic field in multiple dimensions [37]–[41]. If a similar multi-dimensional detection of the marker is developed, it is expected to be helpful for localizing the lesion more precisely. However, since an array of many hall sensors [37]–[40] or several large-sized coils for multi-dimensional detection [41], they are not easy to be integrated into an LP, whose dimension is strictly limited by 10-mm laparoscopy trocar ports. In the development of multi-dimensional lesion localization systems, miniaturization of a hall sensor array or coils would be a challenge.

V. CONCLUSION

In this paper, we proposed an LLS achieving a longer detection range with high precision by using an improved magnetometer that performs baseline cancellation in real-time. The proposed magnetometer, which includes two Hall sensors, can detect small changes of the B field by removing the fluctuating baseline mainly caused by external environments. As a result, the proposed LLS achieved a longer detection range of 40 mm even with a weak magnet, which has a small size with radius = 2.2 mm and thickness = 4.5 mm. This marker is small enough to be handled by commercial clip appliers. An error of less than 0.1% was achieved at a distance of 40 mm, and the maximum error was kept below 6% even when the rotation angle was changed. The proposed LLS achieved a longer detection range than previous LLSs based on RFID. In addition, the proposed LLS does not require any battery, enabling further miniaturization of the marker. It does not involve any external coil, offering a simple setup for the use of LLS during surgery.

REFERENCES

[1] P. Puangmali, K. Althoefer, L. D. Seneviratne, D. Murphy, and P. Dasgupta, "State-of-the-art in force and tactile sensing for minimally invasive surgery," *IEEE Sensors J.*, vol. 8, no. 4, pp. 371–381, Apr. 2008.

[2] G. Niu, B. Pan, Y. Fu, and C. Qu, "Development of a new medical robot system for minimally invasive surgery," *IEEE Access*, vol. 8, pp. 144136–144155, 2020.

[3] X. Tian and Y. Xu, "Low delay control algorithm of robot arm for minimally invasive medical surgery," *IEEE Access*, vol. 8, pp. 93548–93560, 2020.

[4] N. Bandari, J. Dargahi, and M. Packirisamy, "Tactile sensors for minimally invasive surgery: A review of the State-of-the-art, applications, and perspectives," *IEEE Access*, vol. 8, pp. 7682–7708, 2020.

[5] Y. Wada, N. Miyoshi, S. Fujino, M. Ohue, M. Yasui, Y. Takahashi, H. Takahashi, J. Nishimura, Y. Takenaka, K. Saso, A. Tomokuni, K. Sugimura, H. Akita, H. Takahashi, S. Kobayashi, T. Omori, H. Miyata, and M. Yano, "New marking method involving a light-emitting diode and power source device to localize gastrointestinal cancer in laparoscopic surgery," *Sci. Rep.*, vol. 9, no. 1, Apr. 2019, Art. no. 5485.

[6] H. Y. Joo, B. E. Lee, C. I. Choi, D. H. Kim, G. H. Kim, T. Y. Jeon, D. H. Kim, and S. Ahn, "Tumor localization using radio-frequency identification clip marker: Experimental results of an ex vivo porcine model," *Surg. Endoscopy*, vol. 33, no. 5, pp. 1441–1450, May 2019.

[7] C. Shi, M. Li, C. Lv, J. Li, and S. Wang, "A high-sensitivity fiber Bragg grating-based distal force sensor for laparoscopic surgery," *IEEE Sensors J.*, vol. 20, no. 5, pp. 2467–2475, Mar. 2020.

[8] S. Kitano, N. Shiraishi, K. Fujii, K. Yasuda, M. Inomata, and Y. Adachi, "A randomized controlled trial comparing open vs laparoscopy-assisted distal gastrectomy for the treatment of early gastric cancer: An interim report," *Surgery*, vol. 131, no. 1, pp. S306–S311, Jan. 2002.

[9] H. Hayashi, T. Ochiai, H. Shimada, and Y. Gunji, "Prospective randomized study of open versus laparoscopy-assisted distal gastrectomy with extraperigastric lymph node dissection for early gastric cancer," *Surg. Endoscopy*, vol. 19, no. 9, pp. 1172–1176, Sep. 2005.

[10] J. M. C. Yeung, C. Maxwell-Armstrong, and A. G. Acheson, "Colonic tattooing in laparoscopic surgery–making the mark?" *Colorectal Disease*, vol. 11, no. 5, pp. 527–530, Jun. 2009.

[11] M. Montorsi, E. Opocher, R. Santambrogio, P. Bianchi, C. Faranda, P. Arcidiacono, G. R. Passoni, and F. Cosentino, "Original technique for small colorectal tumor localization during laparoscopic surgery," *Diseases Colon Rectum*, vol. 42, no. 6, pp. 819–822, Jun. 1999.

[12] W. J. Choi, J.-H. Moon, J. S. Min, Y. K. Song, S. A. Lee, J. W. Ahn, S. H. Lee, and H. C. Jung, "Real-time detection system for tumor localization during minimally invasive surgery for gastric and colon cancer removal: *In vivo* feasibility study in a swine model," *J. Surg. Oncol.*, vol. 117, no. 4, pp. 699–706, Mar. 2018.

[13] F. Kojima, T. Sato, S. Tsunoda, H. Takahata, M. Hamaji, T. Komatsu, M. Okada, T. Sugiura, O. Oshiro, Y. Sakai, H. Date, and T. Nakamura, "Development of a novel marking system for laparoscopic gastrectomy using endoclips with radio frequency identification tags: Feasibility study in a canine model," *Surg. Endoscopy*, vol. 28, no. 9, pp. 2752–2759, Sep. 2014.

[14] J. L. Ponsky and J. F. King, "Endoscopic marking of colonic lesions," *Gastrointestinal Endoscopy*, vol. 22, no. 1, pp. 42–43, Aug. 1975.

[15] P. Salomon, J. S. Berner, and J. D. Waye, "Endoscopic India ink injection: A method for preparation, sterilization, and administration," *Gastrointestinal Endoscopy*, vol. 39, no. 6, pp. 803–805, Jan. 1993.

[16] K.-I. Fu, T. Fujii, S. Kato, Y. Sano, I. Koba, K. Mera, H. Saito, T. Yoshino, M. Sugito, and S. Yoshida, "A new endoscopic tattooing technique for identifying the location of colonic lesions during laparoscopic surgery: A comparison with the conventional technique," *Endoscopy*, vol. 33, no. 8, pp. 687–691, Aug. 2001.

[17] P. Dell'Abate, A. Iosca, A. Galimberti, P. Piccolo, P. Soliani, and E. Foggi, "Endoscopic preoperative colonic tattooing: A clinical and surgical complication," *Endoscopy*, vol. 31, no. 3, pp. 271–273, Mar. 1999.

[18] S. H. Lee, D. Y. Kim, S. Y. Oh, K. J. Lee, and K. W. Suh, "Preoperative localization of early colorectal cancer or a malignant polyp by using the patient's own blood," *Ann. Coloproctol.*, vol. 30, no. 3, pp. 115–117, Jun. 2014.

[19] N. Miyoshi, M. Ohue, S. Noura, M. Yano, Y. Sasaki, K. Kishi, T. Yamada, I. Miyashiro, H. Ohigashi, H. Iishi, O. Ishikawa, and S. Imaoka, "Surgical usefulness of indocyanine green as an alternative to India ink for endoscopic marking," *Surg. Endoscopy*, vol. 23, no. 2, pp. 347–351, Feb. 2009.

[20] Y. Choi, K. G. Kim, J. K. Kim, K. W. Nam, H. H. Kim, and D. K. Sohn, "A novel endoscopic fluorescent clip for the localization of gastrointestinal tumors," *Surg. Endoscopy*, vol. 25, no. 7, pp. 2372–2377, Jul. 2011.

[21] H. Takeyama, T. Hata, J. Nishimura, R. Nonaka, M. Uemura, N. Haraguchi, I. Takemasa, T. Mizushima, H. Yamamoto, Y. Doki, and M. Mori, "A novel endoscopic fluorescent clip visible with near-infrared imaging during laparoscopic surgery in a porcine model," *Surg. Endoscopy*, vol. 28, no. 6, pp. 1984–1990, Jun. 2014.

[22] S. Narihiro, M. Yoshida, H. Ohdaira, T. Sato, D. Suto, S. Hoshimoto, N. Suzuki, R. Marukuchi, T. Kamada, H. Takeuchi, and Y. Suzuki, "A novel fluorescent marking clip for laparoscopic surgery of colorectal cancer: A case report," *Int. J. Surg. Case Rep.*, vol. 64, pp. 170–173, Oct. 2019.

[23] M. Keskilammi, L. Sydänheimo, and M. Kivikoski, "Radio frequency technology for automated manufacturing and logistics control. Part 1: Passive RFID systems and the effects of antenna parameters on operational distance," *Int. J. Adv. Manuf. Technol.*, vol. 21, nos. 10–11, pp. 769–774, Jul. 2003.

[24] Z. Tang, Y. He, Z. Hou, and B. Li, "The effects of antenna properties on read distance in passive backscatter RFID systems," in *Proc. Int. Conf. Netw. Secur., Wireless Commun. Trusted Comput.*, Apr. 2009, pp. 120–123.

[25] A. Choudhary, D. Sood, and C. C. Tripathi, "Wideband long range, radiation efficient compact UHF RFID tag," *IEEE Antennas Wireless Propag. Lett.*, vol. 17, no. 10, pp. 1755–1759, Oct. 2018.

[26] H. Takahata, F. Kojima, M. Okada, T. Sugiura, T. Sato, and O. Oshiro, "Thoracoscopic surgery support system using passive RFID marker," in *Proc. Annu. Int. Conf. IEEE Eng. Med. Biol. Soc.*, Aug. 2012, pp. 183–186.
[27] T. Ohdaira and H. Nagai, "Intraoperative localization of early-stage upper gastrointestinal tumors using a magnetic marking clip–detecting system," *Surg. Endoscopy*, vol. 21, no. 5, pp. 810–815, Apr. 2007.
[28] H. Xie, T. Gu, X. Tao, H. Ye, and J. Lu, "A reliability-augmented particle filter for magnetic fingerprinting based indoor localization on smartphone," *IEEE Trans. Mobile Comput.*, vol. 15, no. 8, pp. 1877–1892, Aug. 2016.
[29] Y. Zou, G. Wang, K. Wu, and L. Ni, "SmartScanner: Know more in walls with your smartphone!" *IEEE Trans. Mobile Comput.*, vol. 15, no. 11, pp. 2865–2877, Nov. 2016.
[30] T.-H. Chiang, Z.-H. Sun, H.-R. Shiu, K. C.-J. Lin, and Y.-C. Tseng, "Magnetic field-based localization in factories using neural network with robotic sampling," *IEEE Sensors J.*, vol. 20, no. 21, pp. 13110–13118, Nov. 2020.
[31] G. Wang, X. Wang, J. Nie, and L. Lin, "Magnetic-based indoor localization using smartphone via a fusion algorithm," *IEEE Sensors J.*, vol. 19, no. 15, pp. 6477–6485, Aug. 1, 2019.
[32] I. Ashraf, S. Hur, and Y. Park, "mPILOT-magnetic field strength based pedestrian indoor localization," *Sensors*, vol. 18, no. 7, p. 2283, 2018.
[33] Z. Liu, L. Zhang, Q. Liu, Y. Yin, L. Cheng, and R. Zimmermann, "Fusion of magnetic and visual sensors for indoor localization: Infrastructure-free and more effective," *IEEE Trans. Multimedia*, vol. 19, no. 4, pp. 874–888, Apr. 2017.
[34] J. M. Camacho and V. Sosa, "Alternative method to calculate the magnetic field of permanent magnets with azimuthal symmetry," *Revista Mexicana Física*, vol. 59, no. 1, pp. 8–17, Jun. 2013.
[35] J. A. Ajani, "Gastric cancer," *J. Nat. Comput. Cancal Netw.*, vol. 8, no. 4, pp. 378–409, Apr. 2010.
[36] Japanese Gastric Cancer Association, "Japanese gastric cancer treatment guidelines 2010 (ver. 3)," *Gastric Cancer*, vol. 14, no. 2, pp. 113–123, Jun. 2011.
[37] D. Son, S. Yim, and M. Sitti, "A 5-D localization method for a magnetically manipulated untethered robot using a 2-D array of Hall-effect sensors," *IEEE/ASME Trans. Mechatronics*, vol. 21, no. 2, pp. 708–716, Apr. 2016.
[38] S. Song, X. Qiu, J. Wang, and M. Q.-H. Meng, "Real-time tracking and navigation for magnetically manipulated untethered robot," *IEEE Access*, vol. 4, pp. 7104–7110, 2017.
[39] S. Song, X. Qiu, W. Liu, and M. Q.-H. Meng, "An improved 6-D pose detection method based on opposing-magnet pair system and constraint multiple magnets tracking algorithm," *IEEE Sensors J.*, vol. 17, no. 20, pp. 6752–6759, Oct. 2017.
[40] M.-C. Kim, E.-S. Kim, J.-O. Park, E. Choi, and C.-S. Kim, "Robotic localization based on planar cable robot and Hall sensor array applied to magnetic capsule endoscope," *Sensors*, vol. 20, no. 20, p. 5728, Oct. 2020.
[41] S.-L. Liu, J. Kim, B. Kang, E. Choi, A. Hong, J.-O. Park, and C.-S. Kim, "Three-dimensional localization of a robotic capsule endoscope using magnetoquasistatic field," *IEEE Access*, vol. 8, pp. 141159–141169, 2020.

SOON-JAE KWEON (Member, IEEE) received the B.S. and Ph.D. degrees in electrical engineering from Korea Advanced Institute of Science and Technology (KAIST), Daejeon, South Korea, in 2010 and 2018, respectively.

He was a Postdoctoral Researcher with the Information Engineering and Electronics Research Institute, KAIST, from 2018 to 2020. After finishing the first Postdoctoral Research, he is currently with New York University Abu Dhabi, United Arab Emirates, as a Postdoctoral Associate. His research interests include designing low-power sensor interface ICs, wireless communication ICs, data converters for miniature biomedical devices, and wireless sensor nodes.

WOOJIN YUN received the Ph.D. degree in electrical engineering from Chungnam National University, in 2020.

He was with Knowledge on Semiconductor, from 2003 to 2005, as a member of an RF Device Engineer. He was involved in modeling passive devices, designing CDMA power amplifiers, and front-end modules (FEM). From 2006 to 2012, he was with PHYCHIPS Inc., Daejeon, where he developed RFIC transceivers for DSRC systems. He was also involved in the design of TX front-end ICs for wireless communications, including up-conversion mixers, power amplifiers, and baluns. Since July 2012, he has been with the National Nanofab Center (NNFC), Daejeon, South Korea, as a Senior Researcher. His current research interests include biosensors, bioelectronic systems, and MEMS sensors.

HYUNWOO PARK (Student Member, IEEE) received the B.S. degree in electrical and computer engineering from Ajou University, Suwon, South Korea, in 2014, and the M.S. degree in electrical engineering from Korea Advanced Institute of Science and Technology (KAIST), Daejeon, South Korea, in 2017, where he is currently pursuing the Ph.D. degree in electrical engineering. His research interests include circuits and systems for wireless sensor nodes, including data processing algorithms.

JEONG-HO PARK received the B.S. degree in electrical engineering from Korea Aerospace University, Goyang, South Korea, in 2010, and the M.S. and Ph.D. degrees in electrical engineering from Korea Advanced Institute of Science and Technology (KAIST), Daejeon, South Korea, in 2012 and 2017, respectively.

Since 2017, he has been a Staff Engineer with Samsung Electronics Company Ltd. His research interests include designing gas sensor ICs, biosensor ICs, and image sensor systems.

JUNG HOON LEE (Member, IEEE) received the B.S. and M.S. degrees in electrical communications engineering and the Ph.D. degree in electrical engineering from Korea Advanced Institute of Science and Technology (KAIST), Daejeon, South Korea, in 2006, 2008, and 2013, respectively.

He was a Postdoctoral Research Scholar at KAIST, from September 2013 to April 2014, and a Postdoctoral Research Scholar with North Carolina State University, Raleigh, NC, USA, from August 2014 to August 2015. From September 2015 to August 2016, he was an Assistant Professor with the Department of Electronic Engineering, Jeju National University, Jeju, South Korea. He is currently an Assistant Professor with the Department of Electronics Engineering, Hankuk University of Foreign Studies, Yongin, South Korea. His research interests include interference management, limited feedback, machine learning, and signal processing in communication theory and information theory. He was named as an Exemplary Reviewer of the IEEE TRANSACTIONS ON COMMUNICATIONS, in 2015.

JIN LEE received the B.S., M.S., and Ph.D. degrees in electrical engineering from Korea Advanced Institute of Science and Technology (KAIST), Daejeon, South Korea, in 2001, 2003, and 2008, respectively.

He was a Senior Engineer, from August 2009 to February 2017, and a Principal Engineer with Samsung Electronics Company Ltd., South Korea, from March 2017 to February 2018. He is currently an Associate Professor with the Department of Information and Communication, Pyeongtaek University, Pyeongtaek, South Korea. His research interests include the IoT hardware and embedded software for low power applications and the implementation of algorithms and protocols for digital wireless communication.

MINKYU JE (Senior Member, IEEE) received the M.S. and Ph.D. degrees in electrical engineering and computer science from Korea Advanced Institute of Science and Technology (KAIST), Daejeon, South Korea, in 1998 and 2003, respectively.

In 2003, he joined with Samsung Electronics Company Ltd., Giheung, South Korea, as a Senior Engineer and worked on multi-mode multi-band RF transceiver SoCs for GSM/GPRS/EDGE/WCDMA standards. From 2006 to 2013, he was with the Institute of Microelectronics (IME), Agency for Science, Technology and Research (A*STAR), Singapore. He worked as a Senior Research Engineer, from 2006 to 2007, a member of a Technical Staff, from 2008 to 2011, a Senior Scientist, in 2012, and the Deputy Director, in 2013. From 2011 to 2013, he led the Integrated Circuits and Systems Laboratory, IME, as the Department Head. In IME, he led various projects developing low-power 3-D accelerometer ASICs for high-end medical motion-sensing applications, readout ASICs for nanowire biosensor arrays detecting DNA/RNA and protein biomarkers for point-of-care diagnostics, ultra-low-power sensor node SoCs for continuous real-time wireless health monitoring, and wireless implantable sensor ASICs for medical devices, and low-power radio SoCs and MEMS interface/control SoCs for consumer electronics and industrial applications. He was also the Program Director of Neurodevices Program under A*STAR Science and Engineering Research Council (SERC), from 2011 to 2013, and an Adjunct Assistant Professor with the Department of Electrical and Computer Engineering, National University of Singapore (NUS), from 2010 to 2013. He was an Associate Professor with the Department of Information and Communication Engineering, Daegu Gyenogbuk Institute of Science and Technology (DGIST), South Korea, from 2014 to 2015. Since 2016, he has been an Associate Professor with the School of Electrical Engineering, KAIST. He is currently working as a Distinguished Lecturer of the IEEE Circuits and Systems Society. He is the author of five book chapters and has more than 300 peer-reviewed international conference and journal publications in the areas of sensor interface IC, wireless IC, biomedical microsystem, 3-D IC, device modeling, and nanoelectronics. He has also more than 50 patents issued or filed. His research interests include advanced IC platform development including smart sensor interface ICs and ultra-low-power wireless communication ICs, and microsystem integration leveraging the advanced IC platform for emerging applications, such as intelligent miniature biomedical devices, ubiquitous wireless sensor nodes, and future mobile devices.

Dr. Je has served on a Technical Program Committee and an Organizing Committee for various international conferences, symposiums, and workshops, including IEEE International Solid-State Circuits Conference (ISSCC), IEEE Asian Solid-State Circuits Conference (A-SSCC), and IEEE Symposium on VLSI Circuits (SOVC).

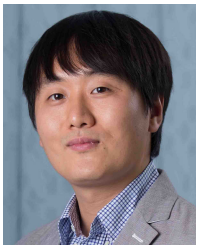

SOHMYUNG HA (Senior Member, IEEE) received the B.S. *(summa cum laude)* and M.S. degrees in electrical engineering from Korea Advanced Institute of Science and Technology (KAIST), Daejeon, South Korea, in 2004 and 2006, respectively, and the M.S. and Ph.D. degrees in bioengineering from the Department of Bioengineering, University of California at San Diego (UCSD), San Diego, La Jolla, CA, USA, in 2015 and 2016, respectively. From 2006 to 2010, he worked with Samsung Electronics Company Ltd., as a Mixed-Signal Circuit Designer for commercial multimedia devices. Since 2016, he has been with New York University Abu Dhabi, United Arab Emirates, and New York University, New York, NY, USA. He is currently an Assistant Professor with New York University Abu Dhabi and a Global Network Assistant Professor with New York University. After this extended career in industry, he returned to academia as a Fulbright Scholar. His research interests include advancing the engineering and applications of silicon integrated technology interfacing with biology in a variety of forms ranging from implantable biomedical devices to unobtrusive wearable sensors.

He is a member of the Analog Signal Processing Technical Committee (ASP TC) and the Biomedical and Life Science Circuits and Systems Technical Committee (BioCAS TC) of the IEEE Circuits and Systems Society (CASS). He has been also a member of the International Technical Program Committee (ITPC) of the International Solid-State Circuits Conference (ISSCC), since 2022. He received a Fulbright Fellowship, in 2010, and the Engelson Best Ph.D. thesis award for biomedical engineering from the Department of Bioengineering, UCSD, in 2016. He served as an Associate Editor for *Smart Health* (Elsevier), from 2016 to 2021. He currently serves as an Associate Editor for IEEE TRANSACTIONS ON BIOMEDICAL CIRCUITS AND SYSTEMS and *Frontiers in Electronics*.

CHOUL-YOUNG KIM (Member, IEEE) received the B.S. degree in electrical engineering from Chungnam National University (CNU), Daejeon, South Korea, in 2002, and the M.S. and Ph.D. degrees in electrical engineering from Korea Advanced Institute of Science and Technology (KAIST), in 2004 and 2008, respectively.

From March 2009 to February 2011, he was a Postdoctoral Research Fellow with the Department of Electrical and Computer Engineering, University of California at San Diego (UCSD), San Diego. He is currently a Professor in electronics engineering with Chungnam National University. His research interests include mm-wave integrated circuits for wireless communication, short-range radar, and phased-array antenna applications.